Optics Letters

Reconfigurable RGB dye lasers based on the laminar flow control in an optofluidic chip

Yue Kong,[1,2] Hailang Dai,[1,2] Xie He,[1,2] Yuanlin Zheng,[1,2,3] and Xianfeng Chen[1,2,4]

[1]The State Key Laboratory on Fiber Optic Local Area Communication Networks and Advanced Optical Communication Systems, School of Physics and Astronomy, Shanghai Jiao Tong University, Shanghai 200240, China
[2]Collaborative Innovation Center of IFSA (CICIFSA), Shanghai Jiao Tong University, Shanghai 200240, China
[3]e-mail: ylzheng@sjtu.edu.cn
[4]e-mail: xfchen@sjtu.edu.cn

Received 9 August 2018; accepted 11 August 2018; posted 17 August 2018 (Doc. ID 342005); published 12 September 2018

The optofluidic dye laser serves as an important on-chip optical source in microfluidic technology for a breadth of applications. One of the ultimate goals of such a light source is an optofluidic white dye laser. However, realizing such a device has been challenging, because it is difficult to achieve simultaneous multi-wavelength lasers that span the most visible spectrum, especially on an integrated system. Here, we demonstrate white lasing in an optofluidic chip that simultaneously lases in red, green, and blue (RGB) colors inside a microfluidic channel. A Fabry–Perot cavity formed by two end-coated fibers provides the optical feedback of the laser. Easy reconfigurable emission can be obtained based on the laminar flow control. Eventually, white lasing at a low threshold was obtained when the pumping energy density is in excess of 26.1 μJ/mm^2.

OCIS codes: (140.0140) Lasers and laser optics; (140.2050) Dye lasers; (140.3410) Laser resonators; (140.3945) Microcavities; (230.3990) Micro-optical devices.

https://doi.org/10.1364/OL.43.004461

Lasers with a wavelength span the full visible spectrum, particularly the red, green, and blue (RGB) colors, have caused much attention in recent years [1–9]. They can be widely used in laser lighting [10,11], laser color imaging and display [12,13], and biological and chemical sensing [14,15]. Recent demonstrations of simultaneous RGB emissions include different types of lasers, for example, semiconductor lasers of RGB lasing in colloidal quantum dot films [2] and the entire visible range from single tricolor nanowires with engineerable bandgaps [16], solid-state lasers of RGB polymer lasing from a free-standing membrane [17], gas lasers of an innovative laser display control technique [18], dye lasers of simultaneous RGB lasing from a single-chip polymer device [19], and white light emission in a disordered system with nanoparticles [4]. However, few of these developments are suitable for integration and spectral tunability at the same time. In addition, some of the devices have difficulties because of their complicated constructions.

In our efforts to achieve such a goal of optical technology, an optofluidic RGB dye laser [20,21] is demonstrated as a feasible and stable approach. An optofluidic dye laser is largely enabled by the recent advances in microfabrication and microfluidics technologies. In many miniaturized systems, microfluidics can manipulate liquids or gases in channels with 10–100 μm dimensions and build the foundation for many chemical, biological, and medical applications. Overall, microfluidics makes it possible to integrate multiple fluidic tasks on a chip while, in most cases, optical components should also be taken into account. Therefore, one advantage of optofluidics is integration which combines optics and microfluidics on the same chip. The other advantage is configurability which illustrates that optical properties can be changed by using manipulating fluids [22].

Optofluidic dye lasers hold great promise as the critical optical source in future integrated optofluidic system. They not only facilitate the implementation of lab-on-a-chip systems, but also allow the dynamic control of laser properties over their solid-state counterparts [23]. Due to a solvatochromic effect, the lasing wavelength and the fluorescence maximum of a certain molecule change with different solvents [24]. Tremendous efforts have been focused on the rapid advancements in the realization of flexible, tunable, and reconfigurable optofluidic microlasers, driven by the growing need for lab-on-a-chip applications. To that end, various configurations have been demonstrated, such as Fabry–Perot (F-P) cavities, distributed feedback Bragg gratings, whispering-gallery cavities, and even random lasing without cavities [25]. The tunability of emission wavelengths is mainly realized by replacing the dye or the solvent, or tuning the period of the Bragg grating by the high elasticity of polymer materials.

In this Letter, we demonstrate a simultaneous and reconfigurable RGB laser device in an optofluidic chip, by taking the advantages of integration of optofluidics and flexibility of the laminar control. The chip is fabricated by conventional soft lithography [26,27] using polydimethylsiloxane (PDMS). This kind of fabrication technique can dramatically reduce the size and complexity of the liquid-handling optical system and is applied to build miniaturized devices with complex

cross-channels which has become the practical assistance for fluidic control and can further regulate the wavelength of visible light. An FP cavity is embedded into a PDMS chip to provide the optical feedback. The gain media used are three kinds of dyes in ethanol solutions, which results in the ease of adjusting lasing characteristics by choosing different dyes. In the experiment, we select stilbene 420 (S-420), coumarin 540 (C-540), and rhodamine 610 (R-610) to achieve the three primary colors of blue, green and red, respectively.

The optofluidic chip design diagram is shown in Fig. 1(a). The microfluidic channel is sandwiched between two layers of PDMS. The channel is 100 μm in width and 125 μm in height. The chip contains inlet ports 1, 2, and 3 for respective injection of R-610, S-420, and C-540. Two outlet ports 1 and 2 are for overflow and keeping systemic liquidity. The pump region, where the stable laminar flow forms, is 5 mm long with two T-junctions at both ends. Two channels (125 μm in width) are placed beside the T-junctions for inserting end-coated fibers as F-P resonator mirrors. The width of the fiber port is the same as the outer diameter of the fiber, which makes sure that the cavity mirrors are paralleled in alignment. To protect the silver film from damage, the fiber ports and T-junctions are designed 30 μm apart. As can be seen from the inset of Fig. 1(b), which is taken by microscope, the coated fibers feature smooth end faces. Once the structure of the chip is given, the only parameter of an F-P cavity that can be adjusted is the reflectivity of the mirrors. A thin layer of Ag is coated to the end faces of multimode fibers with different thicknesses by a vacuum evaporation coating method. The reflectivity of the two fiber-optic reflectors is approximately 85% and 99%.

For the experimental setup in Fig. 1(c), the laser beam incidents on the pump region of a PDMS chip (marked by the dashed rectangle). Meanwhile, dye solutions are injected into the corresponding channels via two syringe pumps (PHD 2000, Harvard apparatus). The syringes of R-610 and S-420 are put on the same pump with united injection velocity. The syringe of C-540 is controlled by the other pump. The emission is detected by an optical fiber spectrometer (AVaSpec 2048-FT, Avantes; spectral resolution = 0.09 nm).

Due to large intensities of pump excitation, dye bleaching should be avoided to increase the lifetime of the component [28]. Thus, we continuously inject dye solutions into the channel. Three dye solutions are also controlled with different injection rates to form a stable laminar flow. The syringe pump allows two syringes at once with a uniform rate. Two of the dye solutions are chosen to be on the same pump. Considering that dye molecular mass and chip inlet positions are influence factors to laminar flow, careful experiments have been tried to find optimized parameters to guarantee a balance among three dye solutions. The optimum solution concentrations have been worked out as S-420 0.75, C-540 0.51 and R-610 1.5 mmol/L. Putting syringes of R-610 and S-420 together on the same pump with injection rate 22 μL/min and C-540 on the other pump with injection rate 15 μL/min, a clear microscope image of stable and uniform laminar flow can be observed in Fig. 2(a). If the injection rate of C-540 is maintained at 15 μL/min, the rate of another two dye solutions can reach up to 25 μL/min; then the variation in laminar flow can be observed in Fig. 2(b). The proportion of dye solutions in the chip channel can be efficiently controlled by manipulating the flow rate. Under the same conditions, when the injection rate of R-610 and S-420 is below 20 μL/min or above 25 μL/min, the three steady laminar flows will be broken and turn into two kinds of laminar flow.

In the beginning, a 405 nm cw (15 mW) laser was chosen as the pump source. Putting three dye solutions in each cuvette and lining them up with direct laser pumping from the left side, as shown in Fig. 3(a), we can get a view of RGB fluorescence emission and a decrease in light intensity with the increase of distance from pumping laser. Under this situation, fluorescence spectra of RGB light were measured to be centered at 627, 521, and 425 nm, as shown in Fig. 3(b). The three dye solutions are injected into a PDMS chip. For the sake of preventing interaction with each other, it is essential to control the flow rate, as mentioned above, to keep a stable flow state. In Fig. 3(c), three pipes can be figured out for injecting dye solutions. Under illuminating, white light beam with RGB light can be clearly seen on chip, which makes preparations for the next step. Dye solutions with different colors can also be spotted on the lower end of the chip owing to constant flow from the outlets.

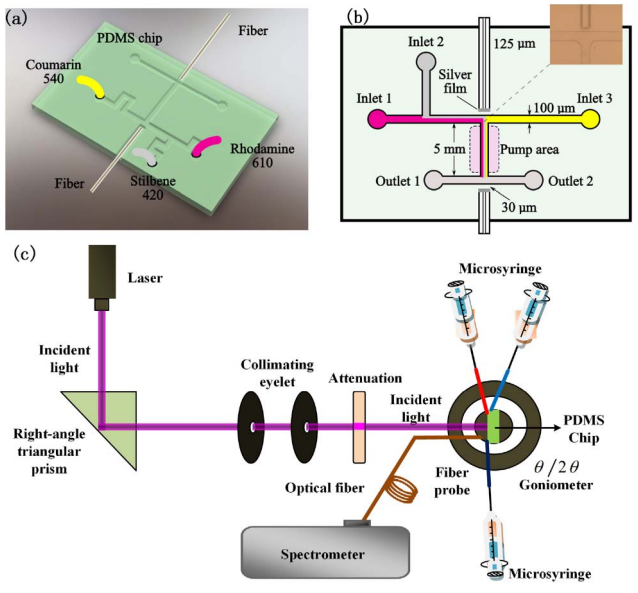

Fig. 1. (a) Chip design diagram. The red, yellow, and gray pipes represent the R-610, C-540, and S-420 injection, respectively. (b) Simplified chip plane schematic diagram. Inset image: the microscope image of a coated fiber and the T-junction. (c) Schematic of the experimental setup.

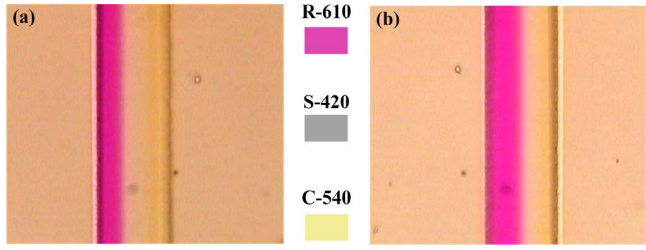

Fig. 2. (a) Microscope image of three laminar flows at the injection rates of R-610 and S-420 at 22 μL/min and C-540 at 15 μL/min. (b) Microscope image of three laminar flows at the injection rates of R-610 and S-420 at 25 and C-540 at 15 μL/min.

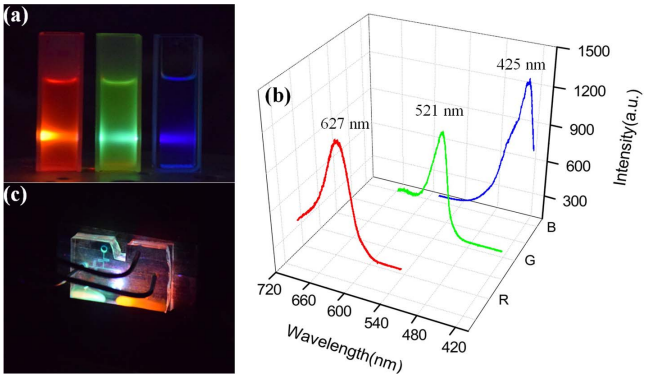

Fig. 3. (a) Cuvettes of three dye solutions with 405 nm CW laser pumping from the left side. (b) 3D fluorescence spectra of red (R), green (G), and blue (B) emission. (c) Image of white light at the pumping region.

To further characterize the lasing properties of our optofluidic device, the chip is optically pumped by the third-harmonic generation of a Nd:YAG laser (355 nm central wavelength, 6 ns pulse width and 20 Hz repetition rate). The emission spectra and chromaticity are shown in Fig. 4, while the emission intensities at different pumping energy densities are shown in Fig. 5. To confirm the lasing action, a detailed analysis is needed. First, the emission intensities of RGB lasers of 355 nm pumping energy densities are provided in Figs. 5(a)–5(c). Red and blue lasers are obtained when pump intensity is 40 μJ/mm^2 and the green laser is obtained at 46 μJ/mm^2. All the spectra are collected using one optical fiber and the intensity of spectra changes with probe points. The low thresholds corresponding to RGB lasers are 16.6, 26.1, and 8.9 μJ/mm^2. Under the same condition, a white light laser can be obtained only when pump intensity is higher than 26.1 μJ/mm^2. Moreover, 2D

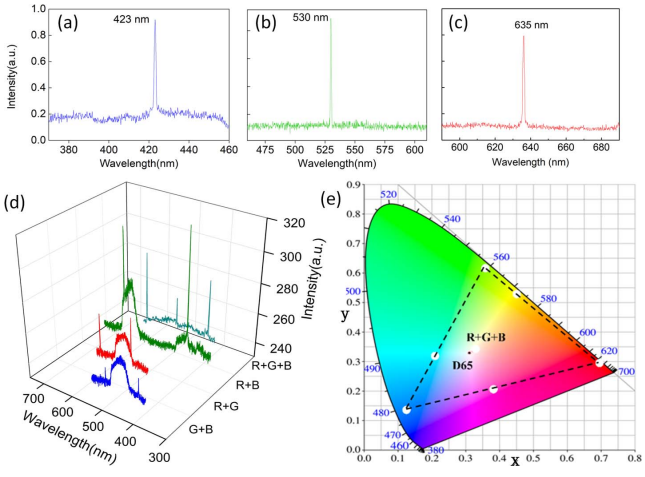

Fig. 4. (a)–(c) Lasing spectra of the RGB laser. (d) Lasing spectra when the green and blue (G + B), red and green (R + G), red and blue (R + B), and red, green, and blue (R + G + B) solutions are pumped above their respective thresholds. (e) Chromaticity of the lasing peaks extracted from the spectra in (a)–(d), and the chromaticity of the R+G+B lasing is close to the CIE standard white illuminant D65. All of these points indicate the range of the achievable color gamut for this white lasing device.

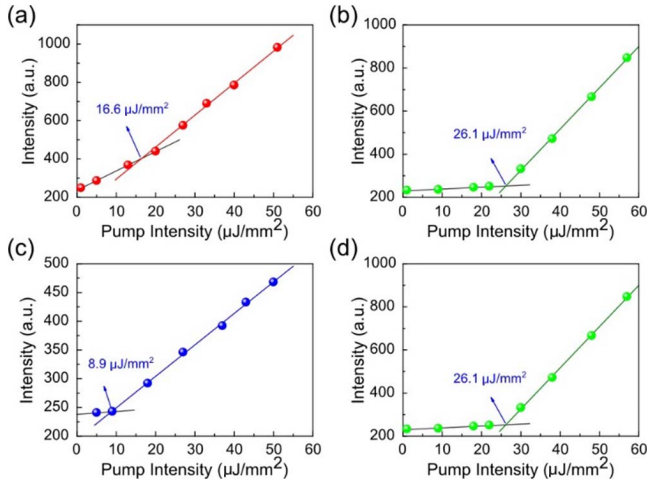

Fig. 5. (a)–(c) Output intensity of the tunable optofluidic laser as a function of the incident pump pulse intensity of the RGB lasing peaks. (d) Using the maximum threshold of a green laser to show a threshold of white lasing.

lasing spectra in Figs. 4(a)–4(c) reveal that a peak wavelength of 635, 521, and 425 nm, with a full width at half-maximum of RGB lasers of 0.6, 0.8, and 0.7 nm, respectively, as is limited by the spectral resolution of the spectrometer. An extremely narrow linewidth has been demonstrated in liquid pulsed dye lasers [29], which shows an improvement opportunity for optofluidic lasers.

By pumping separate injections, two kinds of laminar flows, and three laminar flows of dye solutions, we demonstrate independent lasing of each RGB color, two-color lasing of any two of the three primary colors and, finally, white lasing [shown in Figs. 4(a)–4(d)]. Figure 4(d) presents the emission spectra for all mixed lasing colors. The calculated chromaticity for these lasing spectra on a CIE1931 color diagram by means of white points is given in Fig. 5(e). According to Grassmann's law, a broad range within the diagram inside the triangle formed by the three elementary colors can be realized through appropriate mixing of the three colors. Moreover, the chromaticity of the carefully balanced white lasing point marked with R + G + B is very close to that of the black point in the CIE standard (D65) which provides a proof for the tunability of the white laser.

It is necessary to know that "white laser" does not mean a laser with the color white, but a laser with a wide bandwidth that covers RGB light. We realize both "white" and "lasing" on the integrated PDMS chip. This Letter has greatly simplified the process of the experiment, and it is the first appearance of applying laminar flow to obtain a tunable white lasing.

In summary, we have demonstrated a simultaneous optofluidic white dye laser from an integrated device with a low threshold of 26.1 μJ/mm^2. The key to the demonstration lies in elaborate fabrication of a PDMS chip, appropriate selection of dyes and, most importantly, three steady laminar flows by manipulating the flow rates. The advantages in soft lithography are suitable for integration with other optofluidic networks and largely reduce the hazards of toxic dyes and the complexity in a liquid operation system which moves forward the experimental design. The three different dyes are mutually independent in

the state of laminar flow which, eventually, contributes to a tunable white lasing. The calculated chromaticity of white lasing in the triangle approaches that of the CIE standard white illumination D65 which also underlines the feasibility and reliability of our device.

Funding. National Key R&D Program of China (2017YFA0303700); National Natural Science Foundation of China (NSFC) (11734011, 61405117); Foundation for Development of Science and Technology of Shanghai (17JC1400400).

REFERENCES

1. F. Qian, Y. Li, S. Gradecak, H. G. Park, Y. Dong, Y. Ding, Z. L. Wang, and C. M. Lieber, Nat. Mater. **7**, 701 (2008).
2. C. Dang, J. Lee, C. Breen, J. S. Steckel, S. Coe-Sullivan, and A. Nurmikko, Nat. Nanotechnol. **7**, 335 (2012).
3. X. P. Hu, G. Zhao, Z. Yan, X. Wang, Z. D. Gao, H. Liu, J. L. He, and S. N. Zhu, Opt. Lett. **33**, 408 (2008).
4. S. Chen, X. Zhao, Y. Wang, J. Shi, and D. Liu, Appl. Phys. Lett. **101**, 123508 (2012).
5. K. Fujii, T. Takahashi, and Y. Asami, IEEE J. Quantum Electron. **11**, 111 (1975).
6. J. A. Piper, Opt. Commun. **19**, 189 (1976).
7. B. Abaie, E. Mobini, S. Karbasi, T. Hawkins, J. Ballato, and A. Mafi, Light: Sci. Appl. **6**, e17041 (2017).
8. B. Abaie, T. Hawkins, J. Ballato, and A. Mafi, *Conference on Lasers and Electro-Optics (CLEO)*, OSA Technical Digest (Optical Society of America, 2018), paper FF2H.1.
9. E. Mobini, B. Abaie, M. Peysokhan, and A. Mafi, Opt. Lett. **42**, 1784 (2017).
10. J. J. Wierer, J. Y. Tsao, and D. Sizov, Laser Photonics Rev. **7**, 963 (2013).
11. T. Zhai, Y. Wang, L. Chen, X. Wu, S. Li, and X. Zhang, Nanoscale **7**, 19935 (2015).
12. J. Zhao, H. Jiang, and J. Di, Opt. Express **16**, 2514 (2008).
13. K. Chellappan, E. Erden, and H. Urey, Appl. Opt. **49**, F79 (2010).
14. M. L. Pascu, N. Moise, and A. Staicu, J. Mol. Struct. **598**, 57 (2001).
15. N. A. Naderi, F. Grillot, K. Yang, J. B. Wright, A. Gin, and L. F. Lester, Opt. Express **18**, 27028 (2010).
16. K. Yamashita, N. Takeuchi, K. Oe, and H. Yanagi, Opt. Lett. **35**, 2451 (2010).
17. F. Fan, S. Turkdogan, Z. Liu, D. Shelhammer, and C. Z. Ning, Nat. Nanotechnol. **10**, 796 (2015).
18. Y. Shin, S. Park, Y. Kim, and J. Lee, Opt. Laser Technol. **38**, 266 (2006).
19. Z. Yang, J. Xu, P. Wang, X. Zhuang, A. Pan, and L. Tong, Nano Lett. **11**, 5085 (2011).
20. F. P. Schafer, ed., *Dye Lasers* (Springer, 1990).
21. F. J. Duarte and L. W. Hillman, *Dye Laser Principles* (Academic, 1990).
22. D. Psaltis, S. R. Quake, and C. Yang, Nature **442**, 381 (2006).
23. Z. Li and D. Psaltis, Microfluid. Nanofluid. **4**, 145 (2008).
24. A. J. C. Kuehne, M. C. Gather, I. A. Eydelnant, S. H. Yun, D. A. Weitz, and A. R. Weehler, Lab Chip **11**, 3716 (2011).
25. A. Bakal, C. Vannahme, A. Kristensen, and U. Levy, Appl. Phys. Lett. **107**, 211105 (2015).
26. J. A. Rogers and R. G. Nuzzo, Mater. Today **8**, 50 (2005).
27. G. M. Whitesides, E. Ostuni, S. Takayama, X. Jiang, and D. E. Ingber, Annu. Rev. Biomed. Eng. **3**, 335 (2001).
28. O. Hofmann, X. Wang, A. Cornwell, S. Beecher, A. Raja, D. D. C. Bradley, A. J. Demello, and J. C. Demello, Lab Chip **6**, 981 (2006).
29. F. J. Duarte and J. A. Piper, Appl. Opt. **23**, 1391 (1984).